

A

	Arabidopsis	Rice	Tomato	Maize	Soybean	<i>N. benthamiana</i>
	<i>A. thaliana</i>	<i>O. sativa</i>	<i>S. lycopersicum</i>	<i>Z. mays</i>	<i>G. Max</i>	<i>N. benthamiana</i>
CCT1	AT3G20050	LOC_Os04g46620.1	Solyc01g090750.2.1	GRMZM2G039263_P01	Glyma05g29870.1	Niben101Scf00397g00001.1
				GRMZM2G110626_P01	Glyma08g12970.1	Niben101Scf08606g00014.1
CCT2	AT5G20890	LOC_Os03g42220.1	Solyc11g069000.1.1	GRMZM2G058276_P01	Glyma12g09250.1	Niben101Scf05890g02025.1
		LOC_Os05g48290.3			Glyma11g19220.1	Niben101Scf04560g03018.1
CCT3	AT5G26360	LOC_Os06g34690.1	Solyc05g056310.2.1	GRMZM2G175510_P01	Glyma16g33380.1	Niben101Scf01791g03001.1
		LOC_Os02g14929.1		GRMZM2G069765_P01	Glyma09g28650.2	Niben101Scf32212g00014.1
					Glyma20g35760.1	Niben101Scf04375g08004.1
CCT4	AT3G18190	LOC_Os02g22780.1	Solyc03g118910.1.1	GRMZM2G122767_P01	Glyma08g05470.1	Niben101Scf08653g02001.1
		LOC_Os10g37060.1		GRMZM2G085909_P01	Glyma05g34190.1	Niben101Scf03550g00017.1
					Glyma07g18110.1	
CCT5	AT1G24510	LOC_Os06g36700.1	Solyc05g013990.2.1	GRMZM2G070542_P01	Glyma11g37630.2	Niben101Scf02949g03001.1
				GRMZM2G043383_P01	Glyma18g01580.1	Niben101Scf12680g01003.1
CCT6	AT5G16070	LOC_Os05g05470.1	Solyc02g085790.2.1	GRMZM2G109425_P01	Glyma18g53590.1	Niben101Scf00894g01011.1
	AT3G02530		Solyc02g063090.2.1		Glyma08g47920.1	Niben101Scf02772g05001.1
						Niben101Scf02156g02014.1
CCT7	AT3G11830	LOC_Os06g47320.1	Solyc06g065520.2.1	GRMZM2G009871_P01	Glyma14g04770.1	Niben101Scf06180g00016.1
					Glyma02g44080.1	
CCT8	AT3G03960	LOC_Os03g59020.1	Solyc01g088080.2.1	GRMZM2G083095_P01	Glyma16g26920.1	Niben101Scf12801g00001.1
					Glyma02g07910.1	Niben101Scf03572g02005.1

B

Gene name	Loci number
<i>Tap46</i>	AT5G53000
<i>PPX1</i>	AT4G26720
α -tubulin isoform 6 (<i>TUA6</i>)	AT4G14960
β -tubulin isoform 5 (<i>TUB5</i>)	AT1G20010
β -tubulin isoform 6 (<i>TUB6</i>)	AT5G12250

Supplementary Table S1. Accession and loci numbers of CCT subunit genes (A) and other genes (B) used in this study.

There are eight CCT subunit genes in yeast, while there are nine subunit genes in *Arabidopsis*, tomato, and humans, due to an additional copy of the *CCT6* gene. Other plant species analyzed have higher numbers of CCT subunit genes. There are 11 CCT subunit genes in rice, with two genes each for *CCT2*, *CCT3* and *CCT4*, while there are 12 genes in maize, with two genes each for *CCT1*, *CCT3*, *CCT4*, and *CCT5*. Soybean and *N. benthamiana* respectively have 18 and 17 CCT subunit genes in the genome, more than twice the number of CCT subunit genes in yeast. This may be due to allopolyploidy in soybean and allotetraploidy in *N. benthamiana*.

Supplementary Table S2. List of primers used in this study.

Primer name	Nucleotide sequences (5' → 3')
Primers for GFP-CCTx	
GFP/Flag-CCT1 F	GGA TCC ATG TCG ATC TCC GCC CAA
GFP/Flag-CCT1 R	CCA TGG TTA TTC TTC GCC TTG GCT
GFP/Flag-CCT2 F	GGA TCC ATG CCG ATC GAT AAG ATC
GFP/Flag-CCT2 R	CCA TGG TCA CAT CCT GTC TTC TCT
GFP/Flag-CCT3 F	GGA TCC ATG CAC GCA CCG GTA CTC
GFP/Flag-CCT3 R	CCA TGG TTA GTC GGG AAG AAT TTG
GFP-CCT4 F	CCC GGG AAT GGC GGC GGT AGC GGC A
GFP-CCT4 R	CCC GGG CTA CCT CAC AGT TAC GAT
GFP-CCT5 F	CCC GGG AAT GGC GCT GGC GTT CGA T
GFP-CCT5 R	CCA TGG TCA GTA TTC AGA ATT GGA
GFP-CCT6-1 F	GGA TCC ATG TCA GTG CGA GTT CTG
GFP-CCT6-1 R	ACT AGT TCA AGC AGT AGG CTT CCT
GFP/Flag-CCT6-2 F	GGA TCC ATG TCT GTG CGT GTA CTG
GFP-CCT6-2 R	ACT AGT TTA AGT AGG CTT CCT CAT
GFP-CCT7 F	CCC GGG AAT GGC ATC GAT GAT GCA A
GFP-CCT7 R	CCA TGG TTA TCG CCT TCG CAT TCC
GFP-CCT8 F	GGA TCC ATG GTG GGT ATG TCG ATG
GFP-CCT8 R	ACT AGT TTA GTC TTC CTC CGC ACC

Primers for Flag-CCTx	
Flag-CCT4 F	GAA TTC TAA TGG CGG CGG TAG CGG CA
Flag-CCT4 R	GAA TTC CTA CCT CAC AGT TAC GAT
Flag-CCT5 F	CCC GGG AAT GGC GCT GGC GTT CGA T
Flag-CCT5 R	CCA TGG TAT CAG TAT TCA GAA TTG GA
Flag-CCT6-1 F	GGA TCC ATG TCA GTG CGA GTT CTG
Flag-CCT6-1 R	AGA TCT GTC AAG CAG TAG GCT TCC T
Flag-CCT6-2 R	AGA TCT GTT AAG TAG GCT TCC TCA T
Flag-CCT7 F	CCC GGG AAT GGC ATC GAT GAT GCA A
Flag-CCT7 R	CCA TGG TAT TAT CGC CTT CGC ATT CC
Flag-CCT8 F	GAA TTC TAA TGG TGG GTA TGT CGA TG
Flag-CCT8 R	GAA TTC TTA GTC TTC CTC CGC ACC

Primers for VIGS constructs	
TRV2:CCT2 F	GGA TCC GTT TAT TCT TGA CAA GAA
TRV2:CCT2 R	GGT ACC CTT CTA TAA GCT TGC AAT
TRV2:CCT3 F	GGA TCC GGT AGA CAT TAA AAA GTA
TRV2:CCT3 R	GGT ACC TGT TCA CAA TTA CTG CTC
TRV2:TUA6 F	TCT AGA GAT GTA CCG TGG TGA TGT AGT C
TRV2:TUA6 R/TUA6-Myc R	CCCGGGA GTATTCCTCTCCTTCATC
TRV2:Tap46 F	GGATTCATGGGTGGTTTGGCTATG
TRV2:Tap46 R	GGTACCTTCGATCAGCAGGTGCAC
TRV2:PPX1/2 F	GGA TCC TTC CTG CGG AGA GGA GCT
TRV2:PPX1/2 R	GGT ACC TCC TTC AAA GCC TCG CAG C
TRV2:PPX1/2 mid F	ATT GAG CGA ATC GGA ACA GAG AGT TTG GGG
TRV2:PPX1/2 mid R	CCC CAA ACT CTC TGT TCC GAT TCG CTC AAT

Supplementary Table S2 (Cont.)

Primer name	Nucleotide sequences (5' → 3')
Primers for Myc constructs	
TUA6-Myc F	GTC GAC ATG AGA GAG TGC ATT TCG ATC
TUB5-Myc F	CCC GGG ATG AGA GAG ATC CTT CAC
TUB5-Myc R	CCA TGG TGA GTC TCA TAA TCT CCC TCC
Tap46-Myc F	GAA TTC TAA TGG GTG GTT TGG CTA TG
Tap46-Myc R	CCA TGG TCA GCC ACA AGG TGT GAG
Tap46-N-Myc R	CCA TGG TTC CTT TAT TGC AGA GAG CAT TT
Tap46-C-Myc F	GAA TTC TAA GAC AGT TGA AGG ATG GA
PPX1-Myc F	GTC GAC ATG TCA GAC CTA GAT CGG
PPX1-Myc R	CCC GGG TTA TAG GAA GTA ATC AGG

Primers for BiFC constructs	
CCT2-SPYNE F	CTC GAG ATG CCG ATC GAT AAG ATC
CCT2-SPYNE R	CCC GGG CAT CCT GTC TTC TCT CCT
CCT1-SPYCE F	GTT AAC ATG TCG ATC TCC GCC CAA AAT CC
CCT1-SPYCE R	CCCGGGTTCCTCGCCTTGGCTCTC
CCT3-SPYCE F	CTC GAG ATG CAC GCA CCG GTA CTC
CCT3-SPYCE R	CCC GGG GTC GGG AAG AAT TTG TTC
CCT4-SPYCE F	CCC GGG ATG GCG GCG GTA GCG GCA
CCT4-SPYCE R	CCC GGG CCT CAC AGT TAC GAT GTC
CCT5-SPYCE F	CTC GAG ATG GCG CTG GCG TTC GAT
CCT5-SPYCE R	CCC GGG GTA TTC AGA ATT GGA GAT
CCT6-1-SPYCE F	TCT AGA ATG TCA GTG CGA GTT CTG
CCT6-1-SPYCE R	CCC GGG AGC AGT AGG CTT CCT CAT
CCT6-2 SPYCE F	TCT AGA ATG TCT GTG CGT GTA CTG AA
CCT6-2 SPYCE R	CCC GGG AGT AGG CTT CCT CAT ATT
CCT7 SPYCE F	CTC GAG ATG GCA TCG ATG ATG CAA CCG
CCT7 SPYCE R	CCC GGG TCG CCT TCG CAT TCC ACG
CCT8 SPYCE F	TCT AGA ATG GTG GGT ATG TCG ATG CAG C
CCT8 SPYCE R	ACT AGT GTC TTC CTC CGC ACC AGC AC
Tap46-SPYN/CE F	GGA TCC ATG GGT GGT TTG GCT AT
Tap46-SPYN/CE R	CTC GAG GCC ACA AGG TGT GAG TTT
PPX1-SPYN/CE F	ATC GAT ATG TCA GAC CTA GAT CGG
PPX1-SPYN/CE R	CCC GGG TAG GAA GTA ATC AGG GGC

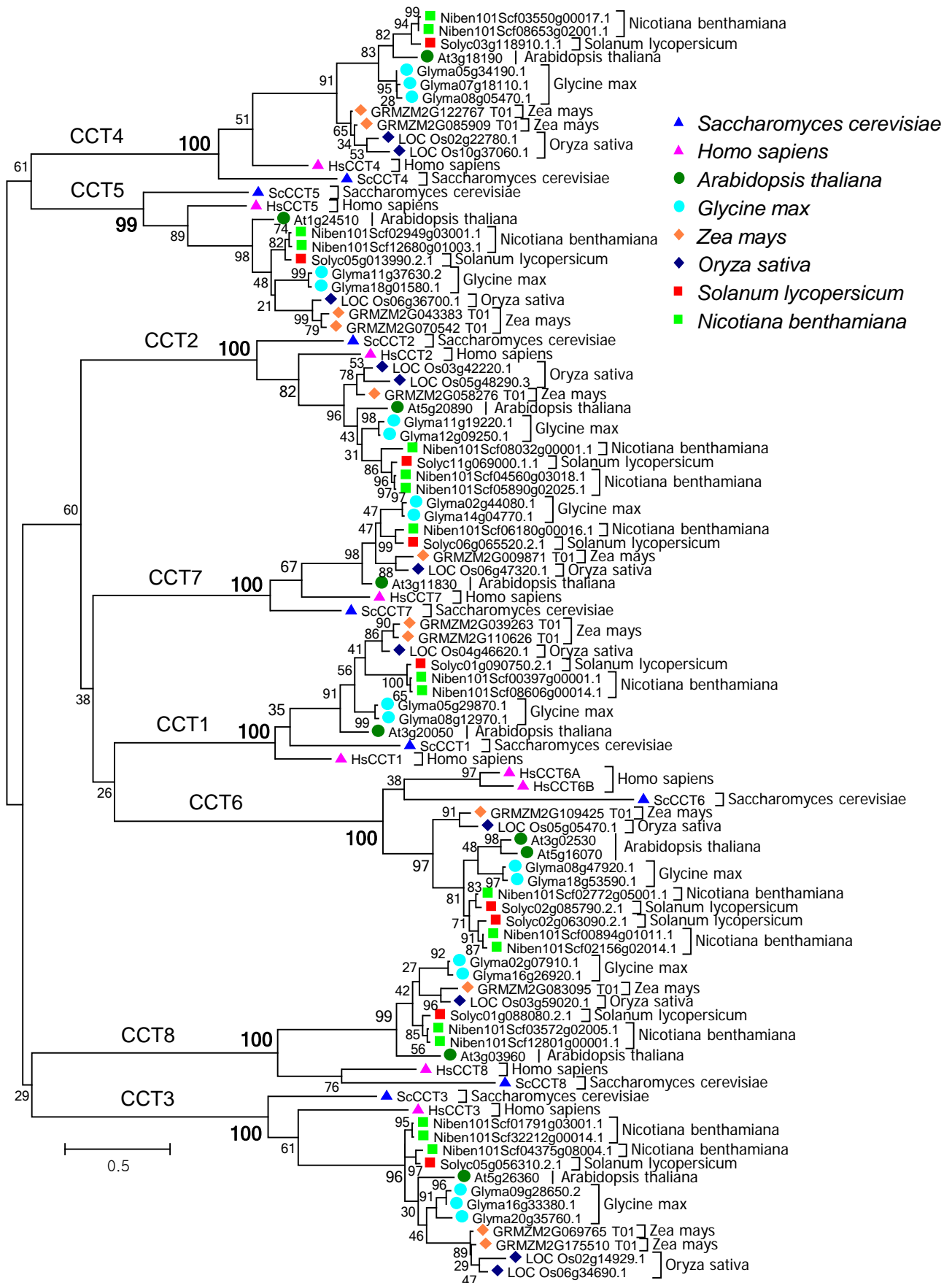
Primers for semi-quantitave RT-PCR	
UBC21 RT-PCR F	CAAGAGCGCGACTGTTTAAA
UBC21 RT-PCR R	TCCTTTCTTAGGCATAGCGG

Primers for Tap46-His recombinant protein	
Tap46-His F	GGA TCC ATG GGT GGT TTG GCT ATG
Tap46-His R	CTC GAG GCC ACA AGG TGT GAG TTT

Supplementary Table S2 (Cont.)

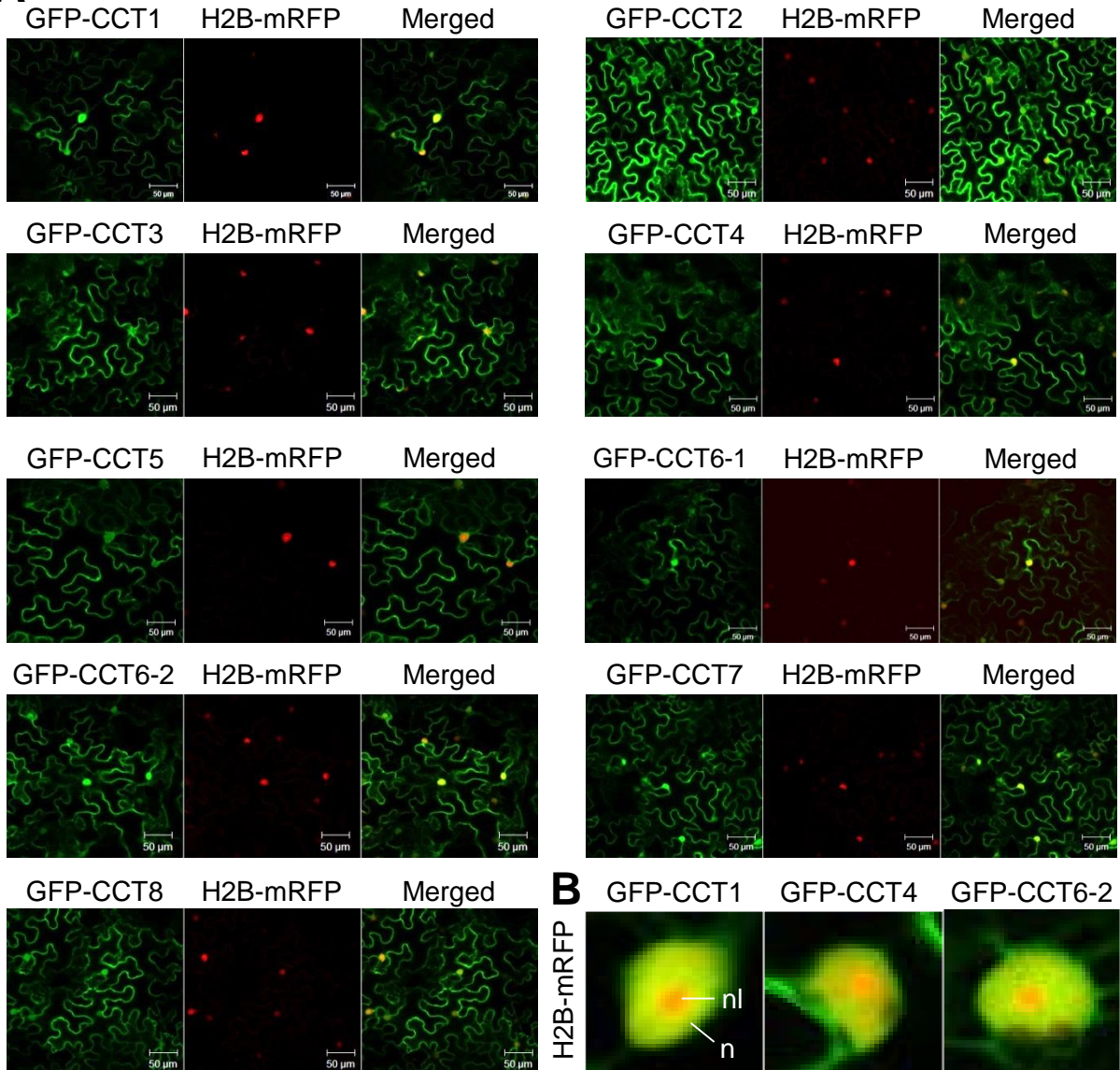
Primer name	Nucleotide sequences (5' → 3')
Primers for RT-qPCR	
CCT1 qPCR F	GTC GGC CTC GAC AAG ATG
CCT1 qPCR R	CGA CCT CCA ACA TCC TAA GAA
CCT2 qPCR F	CTA AGA TTC ACC CTA TGA CCA TCA
CCT2 qPCR R	TTC AGT AAA GCA TTA CGA GCA CA
CCT3 qPCR F	CGC TCA TCC TGC AGC TAA GT
CCT3 qPCR R	ACC AGC TAG AAC AAT AAC AGA CGT T
CCT4 qPCR F	AGT GAG CAA AAG GTT TTT GAT TG
CCT4 qPCR R	ACC GAG CTG CCT TGA GAG
CCT5 qPCR F	TTG CTC ACT TGC GGT TGA T
CCT5 qPCR R	GCA AAC GCC CTA ATT GCA TA
CCT6-1 qPCR F	GAA AGC CTG AGG AAG CTA TTG A
CCT6-1 qPCR R	GAA CAA GCC CCT CAA CCA
CCT6-2 qPCR F	AGT GCC TAA GAC GCT TGC TG
CCT6-2 qPCR R	TCC TTT GTC ATG CTC ACT CG
CCT7 qPCR F	TCC CAA GAC TCC GAG GTG
CCT7 qPCR R	GGC TTC GCT TC TTC AAA
CCT8 qPCR F	GTC GCC CAT TTG AAG CTT AG
CCT8 qPCR R	CTC GTT TCT TGC AAT CGT GA
TUA6 qPCR F	GAA GAA TGT TTC TTA AAA ATT GGA TTT T
TUA6 qPCR R	ACC AGC AAG AGA TAG AAA TAT AGG TTT AG
TUB6 qPCR F	GTG AAA AGA GCT GAT ATT ACC GA
TUB6 qPCR R	TAC ACA CAG ACC ATC ACA AAC AA
PPX1/2 qPCR F	ATT CCG TGT GTT TGA TGC AG
PPX1/2 qPCR R	CGA AGT TTT GCC CAT TAT AGG A
UBC10 qPCR F	ATG GGT CCT TCA GAG AGT CCT
UBC10 qPCR R	CTT GGT CCT AAA GGC CAC CT

Supplementary Figure S1



Supplementary Fig. S1. Phylogenetic tree analysis of CCT subunits.

Phylogenetic tree of CCT subunits were generated using the software MEGA7 (Kumar et al., 2016) with nucleotide sequences from *Saccharomyces cerevisiae*, *Homo sapiens*, *A. thaliana*, *G. max*, *Z. mays*, *O. sativa*, *S. lycopersicum*, and *N. benthamiana*. The tree branches are labeled with a bootstrap score based on 1,000 bootstrap replicates. The branch lengths were measured as the number of substitutions per site. Bootstrap values for each cluster of CCT subunits are shown in *bold*. The scale bar represents 0.5 amino acid substitutions per site in the primary structure.

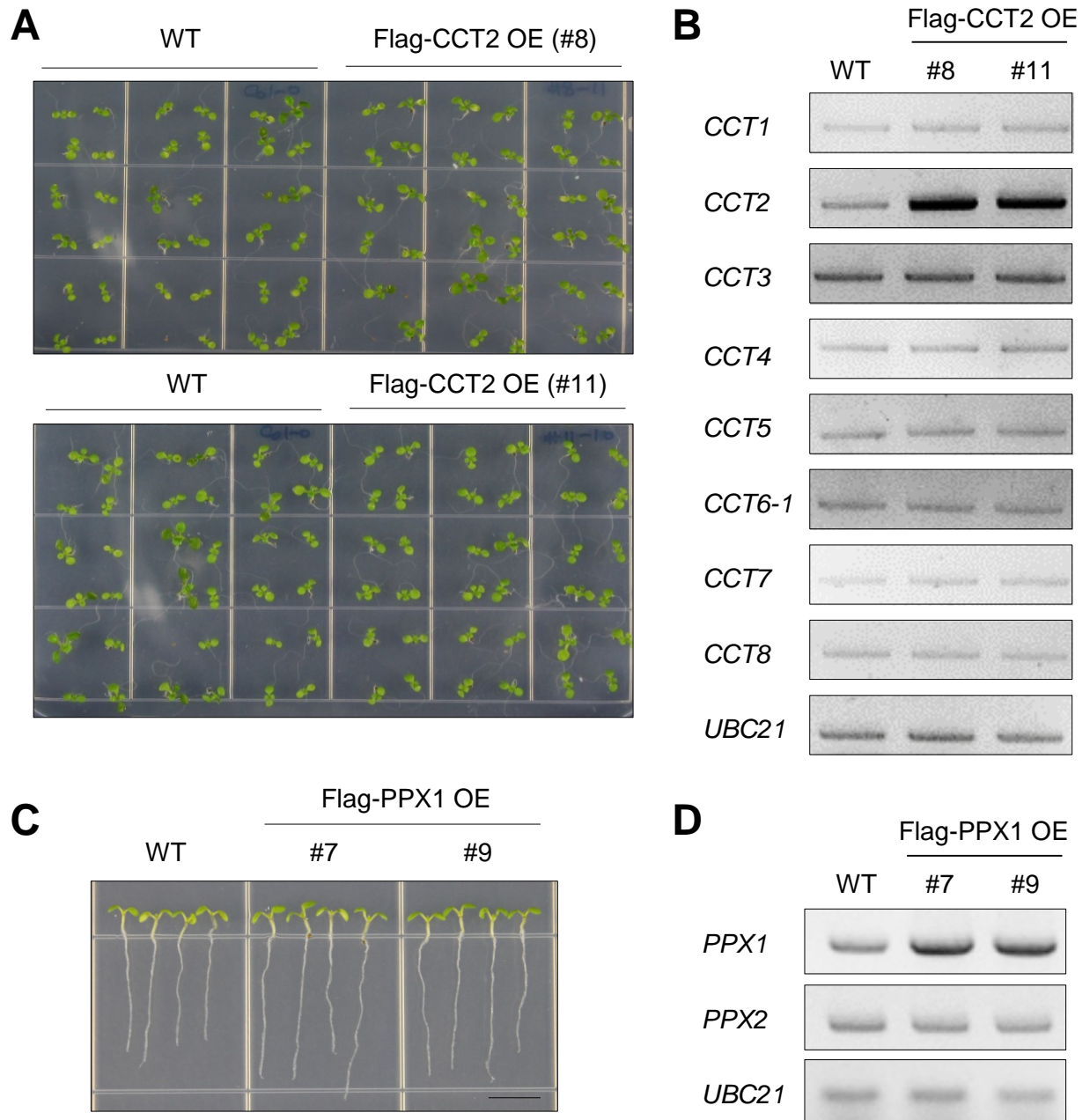
A

Supplementary Fig. S2. Subcellular localization of *Arabidopsis* CCT subunits.

To investigate the cellular functions of the CCT complex in plants, we first determined the subcellular localization of *Arabidopsis* CCT subunits. GFP was fused to the N-terminus of each CCT subunit and transiently expressed in *N. benthamiana* leaves via agroinfiltration, along with mRFP-tagged histone 2B (H2B-mRFP) as a nuclear marker. Confocal laser scanning microscopy of leaf epidermal cells showed that all CCT subunits were mainly localized to the cytosol, but were also detected in the nucleoplasm, but not in the nucleolus. Many of these subunits were predicted to possess nuclear localization signals within their sequences, supporting this observation.

(A) *Arabidopsis* CCT subunits as GFP-fusion proteins were expressed in *N. benthamiana* leaves together with the nuclear marker H2B-mRFP. Fluorescence signals were observed 2 days post-infiltration (DAI). Merged images are shown on the right.

(B) Enlargement of selected images of nuclei from (A). Merged images of GFP-CCT and H2B-mRFP are shown. *n*, nucleus; *nl*, nucleolus.



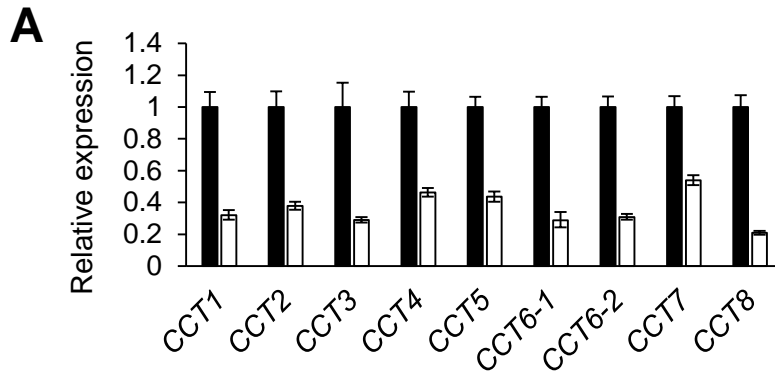
Supplementary Fig. S3. Characterization of *Arabidopsis* Flag-CCT2 overexpression (OE) and Flag-PPX1 OE plants under the control of CaMV35S promoter.

(A) Seedling phenotypes of Flag-CCT2 OE plants (T4 progeny; lines #8 and #11) at 7 days after germination (DAG) in comparison with those of WT (Col-0). The line #8 was used for further analyses.

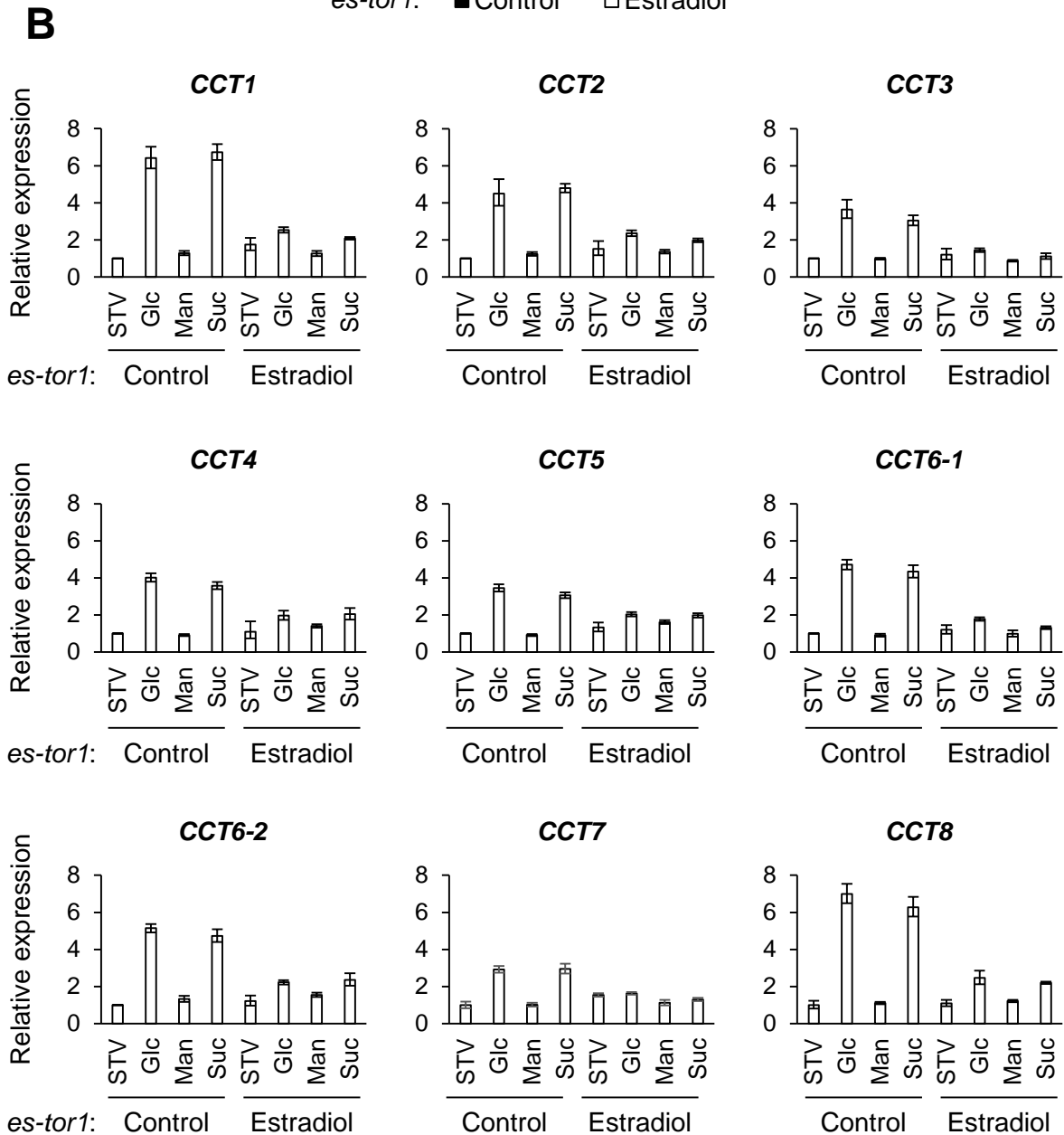
(B) Semi-quantitative RT-PCR of CCT subunit genes in WT and Flag-CCT2 OE (lines #8 and #11) seedlings. *UBC21* mRNA served as the loading control.

(C) Seedling phenotypes of Flag-PPX1 OE plants (T4 progeny; lines #7 and #9) at 7 DAG in comparison with those of WT (Col-0). The line #7 was used for further analyses. Scale bar = 5 mm.

(D) Semi-quantitative RT-PCR of *PPX1* and *PPX2* in WT and Flag-PPX1 OE (lines #7 and #9) seedlings. *UBC21* mRNA served as the loading control.



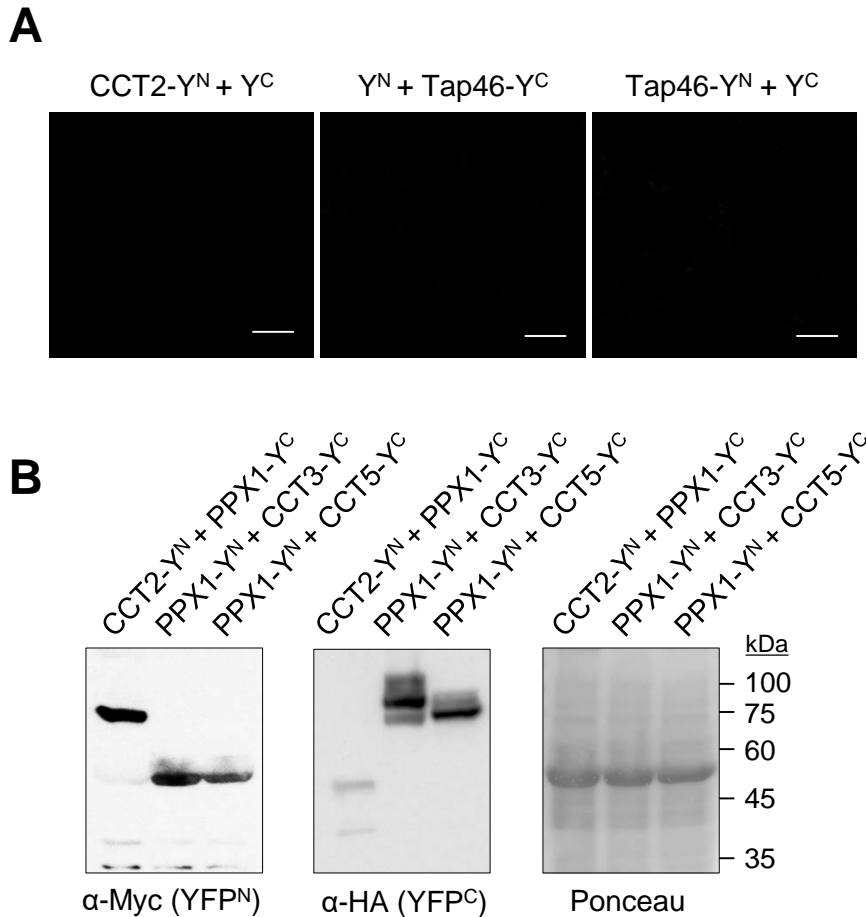
es-tor1: ■ Control □ Estradiol



Supplementary Fig. S4. Expression of *Arabidopsis* CCT subunit genes in estradiol-inducible TOR RNAi (*es-tor1*) plants.

(A) RT-qPCR of CCT subunit genes in TOR-silenced seedlings. The *es-tor1* seedlings were grown for 7 days and treated with ethanol (control) or 10 μ M estradiol for 3 days. Transcript levels are normalized to those of *UBC10* mRNA, and expressed relative to those of control samples. Error bars represent SE from two biological replications. To explore a possible relationship between the CCT complex and the TOR signaling pathway, we tested whether CCT subunit genes are transcriptionally regulated by TOR activity, using *Arabidopsis* estradiol-inducible TOR RNAi (*es-tor1*) lines. Estradiol treatment and subsequent TOR silencing decreased mRNA levels of all CCT subunit genes.

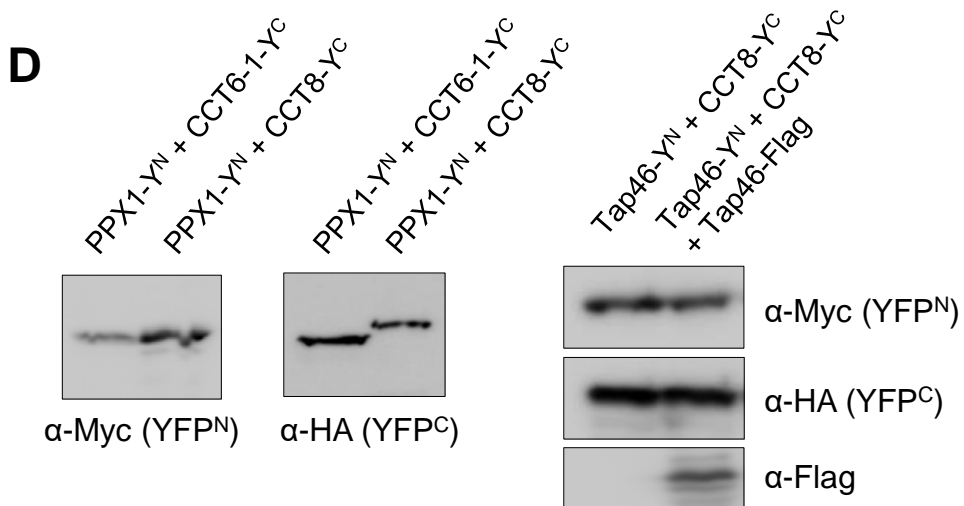
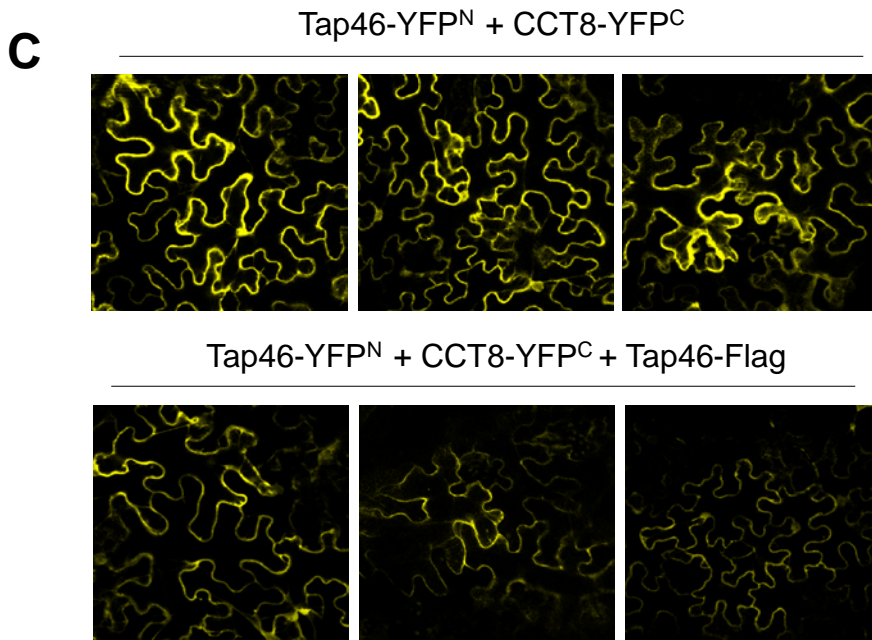
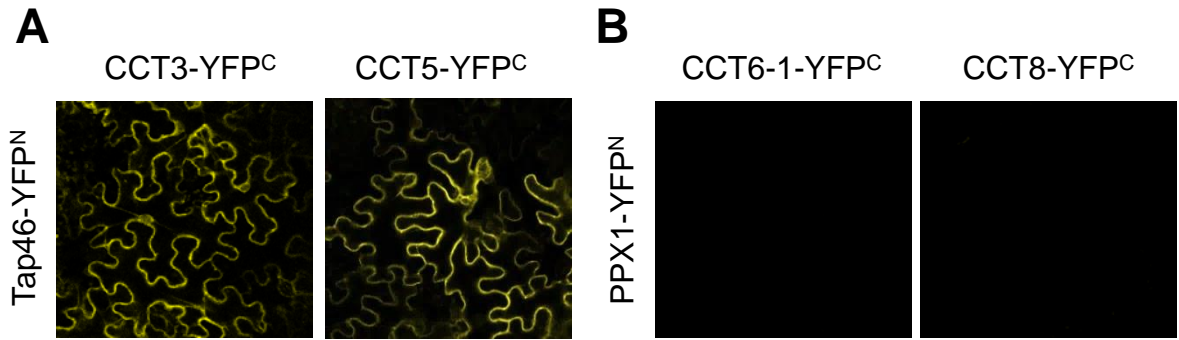
(B) RT-qPCR of CCT subunit genes in TOR-silenced seedlings in response to sugar feeding. The *es-tor1* seedlings grown for 5 days were treated with ethanol (control) or 10 μ M estradiol for 2 days. Then they were transferred to glucose-free medium for 24-h incubation (Stv), and then fed with 30 mM glucose (Glc), mannitol (Man), and sucrose (Suc) for 4 h. Transcript levels are normalized to those of *UBC10* mRNA, and expressed relative to those of Stv samples. Error bars represent SE from two biological replications. Since TOR plays a central role in glucose and energy signaling through rapid transcriptome reprogramming, we tested TOR- and sugar-dependent expression of CCT subunit genes. RT-qPCR analysis revealed that feeding with glucose or sucrose, but not with mannitol, boosted transcription of all CCT subunit genes in control seedlings, suggesting that CCT gene expression is modulated by cellular energy availability. However, TOR silencing by estradiol treatment attenuated the transcriptional changes of the CCT genes. These results suggest that CCT gene expression under normal conditions and in response to sugar feeding is modulated by TOR.



Supplementary Fig. S5. Negative controls and immunoblotting analyses for BiFC experiments shown in Fig. 4B.

(A) Negative control for BiFC. Combinations of CCT2-YFP^N (Y^N) and YFP^C (Y^C), YFP^N and Tap46-YFP^C, and Tap46-YFP^N and YFP^C were expressed in *N. benthamiana* leaves via agroinfiltration. Confocal images were photographed at 2 DAI.

(B) Immunoblotting to detect protein expression in BiFC experiments. YFP^N- and YFP^C-fusion proteins in *N. benthamiana* leaves were detected using anti-Myc and anti-HA antibodies, respectively. Ponceau-stained rbcL served as the loading control.



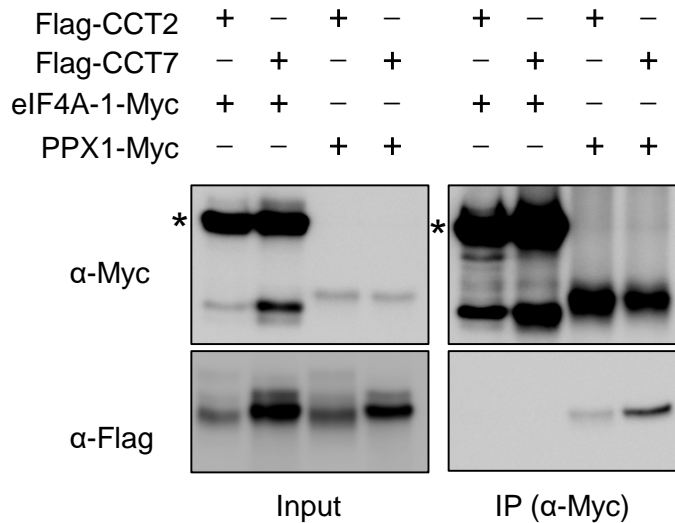
Supplementary Fig. S6. BiFC analyses of CCT interactions with Tap46 and PPX1.

(A) BiFC between Tap46 and CCT subunits. YFP^N and YFP^C constructs were expressed in *N. benthamiana* leaves via agroinfiltration. YFP signals were observed from *N. benthamiana* leaf epidermal cells at 2 DAI by confocal microscopy.

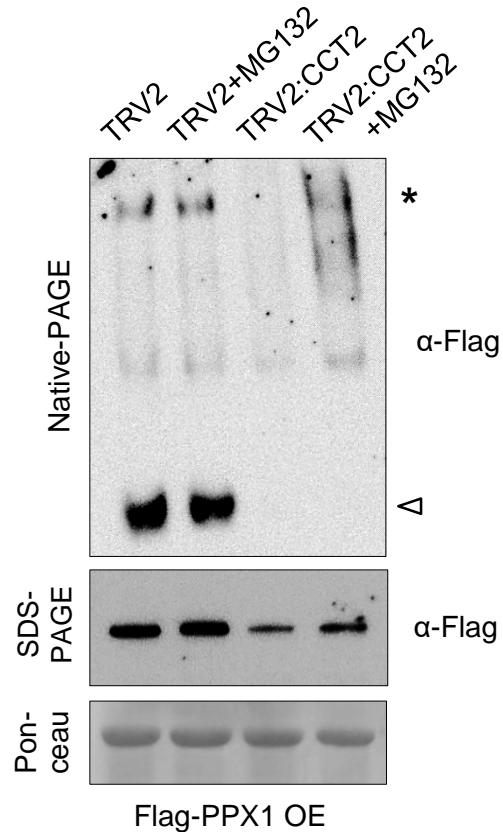
(B) BiFC between PPX1 and CCT subunits. No yellow fluorescence was detected in any combinations.

(C) BiFC between Tap46 and CCT8 with overexpressed Tap46-Flag proteins. Tap46-Flag protein was co-expressed with Tap46-YFP^N and CCT8-YFP^C, which reduced the BiFC signals.

(D) Immunoblotting to detect protein expression in BiFC experiments. YFP^N- and YFP^C-fusion proteins in *N. benthamiana* leaves were detected using anti-Myc and anti-HA antibodies, respectively.

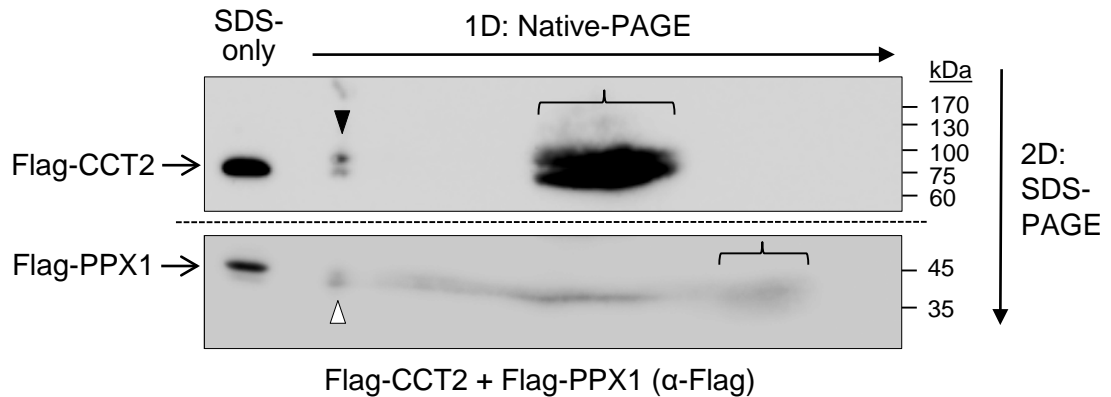


Supplementary Fig. S7. Control experiments for co-IP between PPX1 and CCT subunits. PPX1-Myc and eIF4A-1-Myc were co-expressed with Flag-CCT2 and Flag-CCT7 in *N. benthamiana* leaves. Immunoprecipitation was performed with anti-Myc antibody-conjugated resin, followed by immunoblotting with anti-Myc and anti-Flag antibodies to detect immunoprecipitated and co-immunoprecipitated proteins, respectively. CCT2 and CCT7 were immunoprecipitated with PPX1-Myc, but not with eIF4A-1-Myc (*asterisks*), despite abundant expression and successful immunoprecipitation of eIF4A-1-Myc. These results suggest specific interactions between PPX1 and CCT subunits.



Supplementary Fig. S8. Native-PAGE and SDS-PAGE of Flag-PPX1 OE plants after CCT2 VIGS with or without MG132 treatment.

Immunoblotting was performed with anti-Flag antibody with or without MG132 treatment (20 μ M, 4-h). The *asterisk* and *white arrowhead* indicate the CCT complex-associated form and the mature form of Flag-PPX1, respectively. Ponceau-stained rbcL served as the loading control.



Supplementary Fig. S9. 2-dimensional PAGE using *N. benthamiana* extracts that co-expressed Flag-CCT2 and Flag-PPX1.

After native-PAGE (1D) and SDS-PAGE (2D), immunoblotting was performed with anti-Flag antibody. Flag-CCT2 and Flag-PPX1 detected at the position of the CCT complex are marked with *black* and *white arrowheads*, respectively. Monomeric Flag-CCT2 and Flag-PPX1 are marked with *brackets*. The band intensity of Flag-PPX1 was substantially lower than that of Flag-CCT2, and to match the band intensity between the two proteins, the membrane was cut (*dashed line*) and exposed for different time periods. In the “SDS-only” lane, cell extracts co-expressing Flag-CCT2 and Flag-PPX1 were loaded onto the 2D gel (SDS-PAGE) for immunoblotting to mark the position of Flag-CCT2 and Flag-PPX1.